High-Power Ferrite Circulators*

PETER A. RIZZI†

Summary—**The Faraday rotation and insertion loss of various ferrite-loaded waveguide structures have been studied in order to determine their power-handling capacities. A method of measuring insertion loss to within ±0.05 db is described. Two figures of merit containing this information are defined for the various configurations. The first, defined as the rotation per attenuation, indicates for a given value of rotation the efficiency of power transmission through the device, while the second, defined as the dissipative area per power loss, indicates the power handling capacity of the structure. By utilizing this information, the author has described an *X*-band ferrite circulator which is capable of handling an average power of 1000 watts. In addition, the design of a 2000-watt gyrator type circulator is indicated.**

Introduction

When a dc magnetic field is applied to a waveguide containing a ferrite material, the ferrite responds anisotropically to the rf field. Because of the gyroscopic nature of the electrons which determine the magnetization of the ferrite, a nonsymmetrical tensor is required to describe its rf permeability. This lack of symmetry coupled with the high resistivity of the ferrite implies the possibility of realizing microwave circuit elements which do not obey the law of reciprocity. In recent years, many useful devices have been developed which employ this property. Some of these use the Faraday rotation of an electromagnetic wave in a cylindrical waveguide to obtain their nonreciprocal behavior. For example, Hogan[1] described two types of circulators which employ the ferrite's nonreciprocal property. In many applications, however, the losses in these devices are prohibitively large. Consequently, the associated temperature rise adversely affects the power handling capacity of the device.

Kales[2] has investigated the case of solid ferrite rods in a cylindrical waveguide and obtained characteristic equations which, when solved, determine the propagation constants for the various modes. More recently, Suhl and Walker[3] have studied the propagating modes in a cylindrical ferrite waveguide structure and have also employed perturbation techniques to obtain the propagation constants for a waveguide containing either a very thin pencil of ferrite or a ferrite which was only weakly magnetized. In addition to the above investigations, Sakiotis and Chait[4,5] and Fox, Miller, and Weiss[6] have made an extensive study of the properties of ferrites in waveguides.

The present work considers the case of a cylindrical rod magnetized in the direction of propagation for which curves of rotation and insertion loss have been obtained for various diameters and lengths of ferrite. From this information a figure of merit, defined as the rotation per attenuation, was calculated for the various ferrite diameters. This revealed the ferrite diameter which gave the greatest efficiency of power transmission through the ferrite-loaded guide.

An analysis of a hollow ferrite cylinder in a cylindrical waveguide has been made. Theoretical values of rotation for both the solid and hollow rod case have been calculated. Experimental values of rotation and attenuation have also been obtained. From this data a figure of merit, defined as the dissipative or surface area of the ferrite rod per attenuation, has been determined. This enables one to determine the ferrite geometry for maximum power handling capacity.

Theoretical Results

Polder[7] and Hogan[1] have demonstrated that when an electromagnetic wave is propagated in a ferrite medium which has been magnetized to saturation in the z direction, the rf components of B and H are related by a tensor permeability. By considering the case of uniform plane wave propagating through a ferrite medium magnetized in the direction of propagation, the above investigators showed that the plane of polarization of the wave was rotated as it propagated through the ferrite. The rotation per unit length is related to the propagation constants in the following manner:

$$\theta = \frac{\beta_- - \beta_+}{2} \tag{1}$$

where β_+ and β_- are the propagation constants for the right, and left-hand circularly-polarized waves, respectively.

Using the waveguide analysis described by Kales,[2] the author[8] has derived characteristic equations for the

* Manuscript received by the PGMTT, November 19, 1956; revised manuscript received, June 28, 1957. This paper is based in part on a dissertation submitted in partial fulfillment of the requirements for the Doctor of Eng. degree, Yale University, New Haven, Conn.

† Raytheon Manufacturing Co., Missile Systems Div., Bedford, Mass.

[1] C. L. Hogan, "The microwave gyrator," *Bell Sys. Tech. J.*, vol. 31, pp. 1–31; January, 1952.

[2] M. L. Kales, "Modes in waveguides that contain ferrites," *J. Appl. Phys.*, vol. 24, pp. 604–608; May, 1953.

[3] H. Suhl and L. R. Walker, "Topics in guided wave propagation through gyromagnetic media," *Bell Sys. Tech. J.*, vol. 33, pp. 579–659, and 1133–1194; May and September, 1954.

[4] H. N. Chait and N. G. Sakiotis, "Ferrites at microwaves," PROC. IRE, vol. 41, pp. 87–93; January, 1953.

[5] N. G. Sakiotis and H. N. Chait, "Properties of ferrites in waveguides," IRE TRANS., vol. MTT-1, pp. 11–16; November, 1953.

[6] A. G. Fox, S. E. Miller, and M. T. Weiss, "Behavior and applications of ferrites in the microwave region," *Bell Sys. Tech. J.*, vol. 34, pp. 5–103; January, 1955.

[7] D. Polder, "On the theory of ferromagnetic resonance," *Phil. Mag.*, vol. 40, pp. 99–115; January, 1949.

[8] P. Rizzi, "The electromagnetic field in composite dielectric and ferrite waveguide structures," D.Eng. dissertation submitted to Yale School of Eng., pp. 36, 43; 1955.

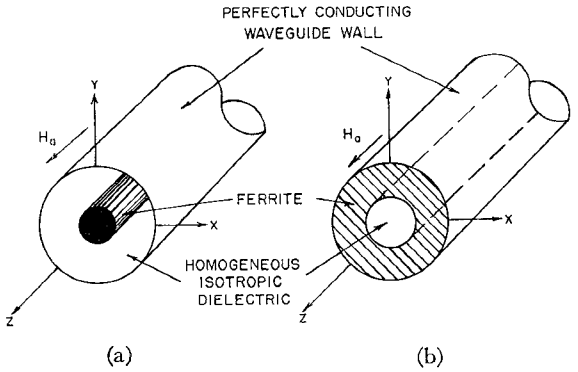

Fig. 1—Composite ferrite and dielectric waveguide structures.

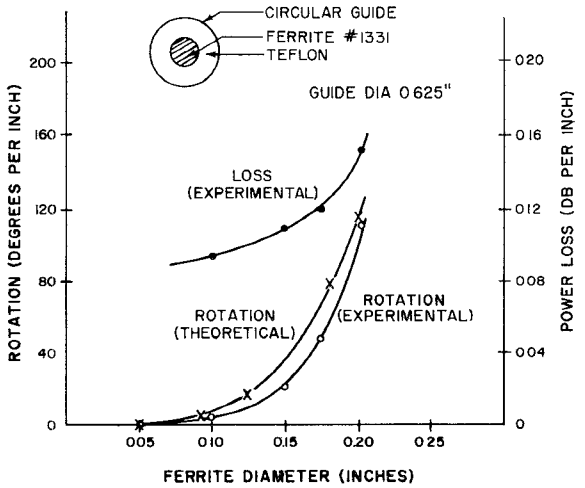

Fig. 2—Saturation rotation and loss for the teflon and ferrite structure shown in Fig. 1(a).

two waveguide configurations shown in Fig. 1. A brief outline of the analysis is given in the Appendix.

Because of the complexity of the characteristic equations, graphical methods were used to solve for the propagation constants of the circularly-polarized waves. Then by use of (1), the rotation per unit length for various ferrite diameters was determined. For the structure shown in Fig. 1(a), the following materials were used:

Ferrite MF-1331[9]

Relative dielectric constant $= \epsilon = 13$.
Saturation magnetization $= M_a = 2200$ Gauss.
(The dc magnetic field was set at 300 oersteds.)

Teflon

Relative dielectric constant $= \epsilon_1 = 2.08$.

Fig. 2 shows the theoretical values of saturation rotation at X band for various ferrite diameters.

For the structure shown in Fig. 1(b), a hollow MF-1331 ferrite cylinder was assumed in the calculations.

[9] Ferrite MF-1331, now designated as R-1, is produced by the General Ceramics Corp., Keasbey, N. J. The above values of dielectric constant and saturation magnetization are typical for MF-1331.

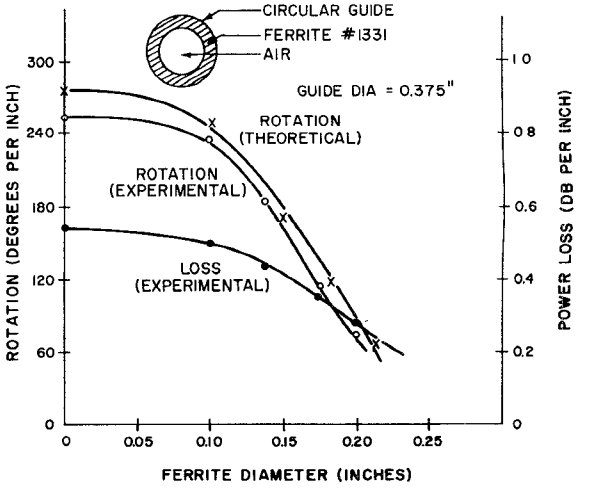

Fig. 3—Saturation rotation and loss for the hollow ferrite structure shown in Fig. 1(b).

The center section contained air so that the relative dielectric constant in this region was unity. Fig. 3 shows the theoretical values of saturation rotation at X band for various inside ferrite diameters. It is interesting to note that with a hole in the center of the ferrite equal to approximately half the waveguide diameter (Fig. 3), one obtains the same amount of rotation as from a solid rod 0.20 inch in diameter placed at the center of the teflon-loaded guide (Fig. 2). This implies that if the losses are of the same order of magnitude in the two structures, the hollow cylinder with its larger dissipative area should be capable of handling much higher amounts of microwave power without having to increase the length of the Faraday rotator. The hollow cylinder has an additional advantage in that the ferrite touches the metallic waveguide wall and consequently can conduct the generated heat away more readily than the solid ferrite rod which is imbedded in teflon.

In order to determine theoretically the attenuation in the ferrite structures, tables of the various type Bessel functions for complex arguments are required. However, since the available tables are not complete enough for our purpose, we must turn to an experimental study of the loss characteristics for the various ferrite configurations.

Experimental Techniques and Results

For the purpose of studying the rotation and loss characteristics in composite ferrite and dielectric waveguide structures, the measuring apparatus shown in Fig. 4 was assembled.

In order to measure the Faraday rotation in the circularly symmetric ferrite structures, a rotary joint and protractor combination was employed. By gradually increasing the magnetic field, the rotation, due to the ferrite, also increased. Thus, by turning the circular-to-rectangular transition at the output of the ferrite section so that the rotation meter always reads a maximum, the rotation can be "followed" as it increases due to the

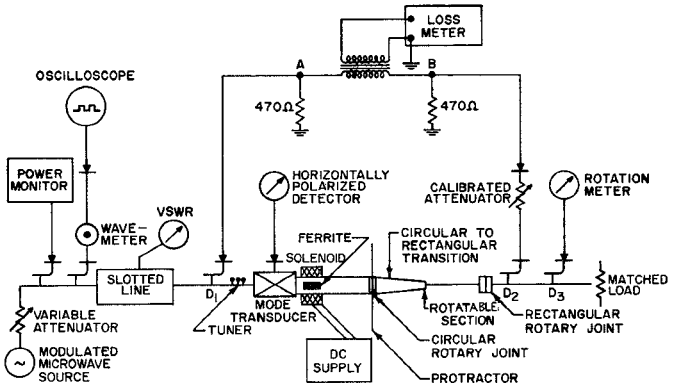

Fig. 4—Apparatus for measuring rotation and loss in ferrites at X band.

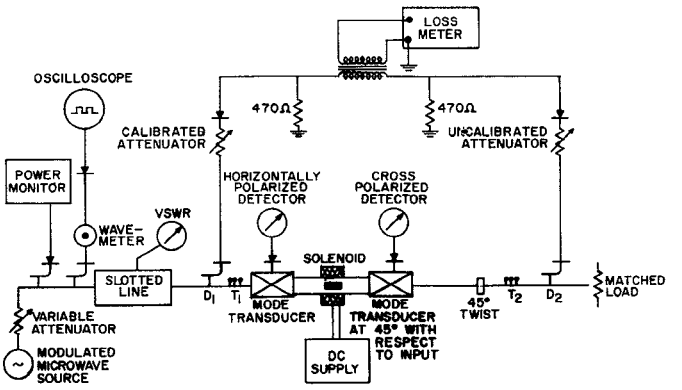

Fig. 5—Improved loss measurement apparatus.

increasing magnetic field. By continuing this process until the ferrite is saturated, the saturation rotation of the sample can be determined. With the circular-to-rectangular transition set for a maximum reading on the rotation meter, the insertion loss due to the ferrite-loaded waveguide structure can be measured. This is accomplished by sampling the input and output energy from directional couplers D_1 and D_2, respectively. The difference between the crystal outputs is fed to a transformer and amplified. The output signal thus indicates the amount of attenuation in the structure between D_1 and D_2. To calibrate the output or loss meter, a calibrated attenuator was inserted in the second or output branch of the circuit as shown in Fig. 4. By placing an air-filled waveguide section between the two directional couplers, the calibrated attenuator was varied until a null was obtained on the loss meter. Thus, with this attenuator setting, the circuit was balanced for zero loss. The loss meter was then calibrated by introducing known amounts of loss with a standard attenuator. With the calibrated attenuator returned to its setting for zero loss and the air-filled waveguide section replaced by the ferrite-loaded guide, the insertion loss for both solid and hollow rod ferrite structures was obtained.

Since the ferrite structures were cylindrical in cross section, a mode transducer was employed to change the dominant TE_{10} mode in rectangular guide to TE_{11} mode in circular guide. In addition to its transducing properties, this device also contains an output terminal which accepts any horizontally-polarized reflections[10] from the ferrite structure. Because of the horizontally-polarized detector's position in the measurement setup, the loss meter actually measures the power absorbed by the ferrite structure plus that absorbed by the horizontally-polarized detector. In order to obtain the actual power loss in the ferrite structure, the apparent power loss due to horizontally-polarized reflections was subtracted from the loss meter reading. Fig. 2 and Fig. 3 show the insertion loss and the measured saturation rotation at X Band for various diameters of solid and holly cylinders of ferrite No. 1331. Comparison with the theoretical curves shows that the measured and computed values of rotation are in agreement to within 10 per cent. The variation in saturation magnetization from the value of 2200 Gauss assumed in the calculations accounts for most of this discrepancy.

By using the improved measurement technique described below, some of the above data were checked. In addition, measurements were made on hollow rod samples with larger inside and outside diameters. The improved loss measurement system is shown in Fig. 5. With a section of essentially lossless waveguide between the directional couplers D_1 and D_2 and the calibrated attenuator set at zero attenuation, the uncalibrated attenuator is adjusted so that the loss meter reads zero. Next, the ferrite section and mode transducers are placed between the directional couplers. By increasing the magnetic field, the rotation is increased to the value of $(N\pi+\pi/4)$ nearest the saturation rotation. A slight adjustment of magnetic field and tuner T_2 will yield nulls in the cross-polarized and horizontally-polarized detectors, respectively. The tuner T_1 is then used to minimize the input vswr. Since the system has been tuned for maximum transmission, the only significant loss is that due to the ferrite section. The final step of the procedure is to adjust the calibrated attenuator so as to renull the loss meter. The amount of loss required to renull is equal to the loss through the ferrite-loaded waveguide section. In all the ferrite structures which were investigated, the cross-polarized detector null was at least 40 db down from the input power level. Thus, the ellipticity introduced by the ferrite section was negligible. The horizontally-polarized detector null was at least 50 db down from the input so that its effect on the loss measurements was also negligible. An analysis of this system and the data obtained from it indicated that the measurement errors were less than ± 0.05 db. Fig. 6 shows some of the loss data obtained on large diameter hollow ferrite rods using the above technique.

From the data in Figs. 2, 3, and 6 curves of Q_T, defined as the rotation per attenuation, and Q_D, defined as the dissipative area per power loss, can be plotted for the various configurations.[11] These are given in Fig. 7–

[10] All reflections were reduced, in part, by use of quarter-wave dielectric transformers on each end of the ferrite cylinders.

[11] The total cylindrical surface of the ferrite is considered as the dissipative area. That is, the dissipative area per unit length is equal to πd for solid cylinder and $\pi(d_{\text{inside}}+d_{\text{outside}})$ for hollow cylinder.

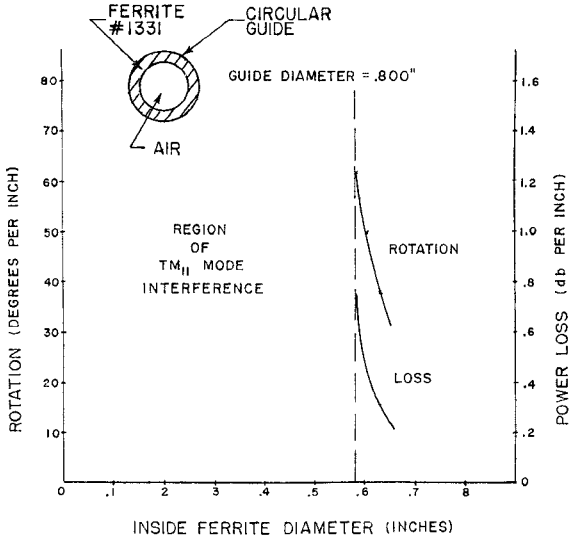

Fig. 6—Saturation rotation and loss for large hollow cylinders.

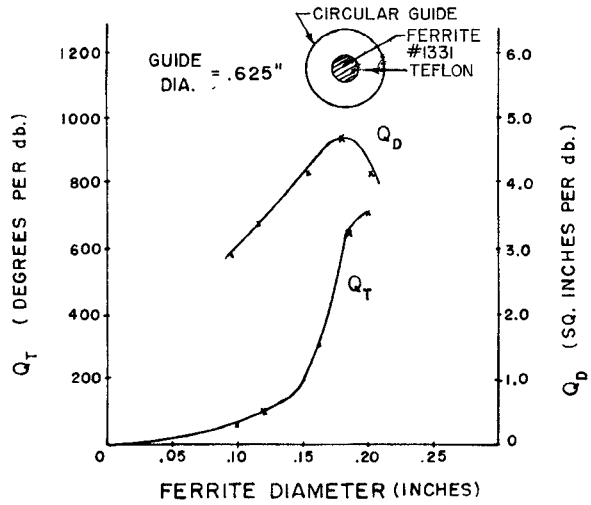

Fig. 7—Figures of merit for teflon and ferrite structures.

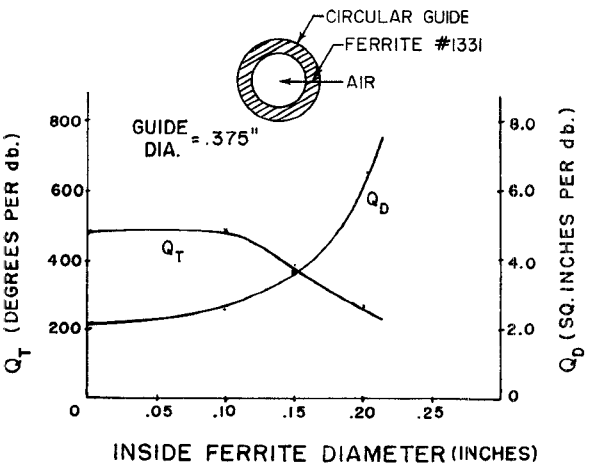

Fig. 8—Figures of merit for small hollow ferrite cylinders.

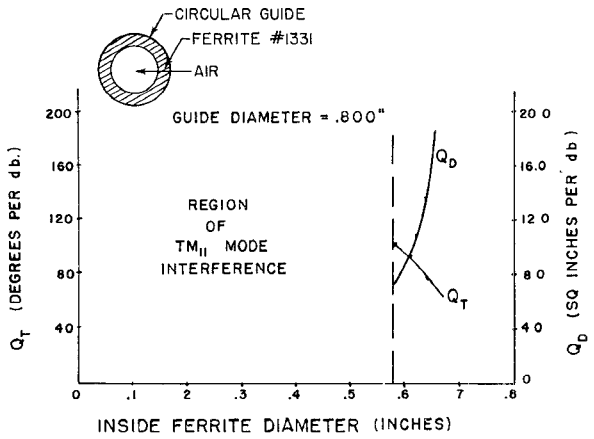

Fig. 9—Figures of merit for large hollow ferrite cylinders.

Fig. 9. Inspection of the Q_T curves for the various configurations indicate that if one is concerned with efficiency of power transfer, the solid rod structures are obviously better. However, more often the problem is one of obtaining a structure with a very large power handling capacity while maintaining the insertion loss reasonably low, but not necessarily at a minimum. For example, if 0.5 db were set as the maximum allowable loss for a ferrite structure with a saturation rotation of 45°, one would be free to choose any structure with a Q_T greater than 90°/db. Since large power handling capacity is desired, one would consequently choose the structure with the highest Q_D. At this point it should be mentioned that the values of Q_D for teflon and ferrite cannot be compared directly with Q_D for the hollow rod case. First of all, the loss curve in Fig. 2, and consequently Q_D in Fig. 7, contains the losses due to the teflon. Secondly, the efficiency of heat transfer from the ferrite to the waveguide wall is different for the two geometries. Therefore, strictly speaking, the Q_D curves are only valuable in determining what dimensions of a given ferrite geometry yield greatest power handling capacity.

Description of High-Power Circulators

A study of the data in the previous section resulted in the choice of the structure in Fig. 10 for use in high-power ferrite circulators. This choice, as previously discussed, amounted to a compromise between high-power handling capacity (Q_D) and low insertion loss(Q_T).

One type of circulator described in the literature[1] employs a pair of two-mode transducers and a ferrite section which gives 45° of Faraday rotation. This type is shown in Fig. 11. Due to the ferrite's rotation, energy entering port 1 travels to port 2 practically unattenuated. Similarly, energy entering port 2 travels to port 3 while energy entering port 3 travels to port 4. This type of circulator has been built at X band with an insertion loss of less than 0.4 db between successive ports and a reverse loss of greater than 20 db over a 5 per cent frequency band. The reverse loss is limited by the frequency sensitivity of the saturation rotation which varies from 40° to 50° over the 5 per cent frequency band. High-power tests have shown this circulator capable of handling at least an average power of 1000 watts with no forced cooling of the ferrite section. Since a higher power

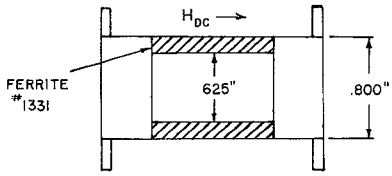

Fig. 10—Hollow ferrite cylinder used in high-power ferrite circulators.

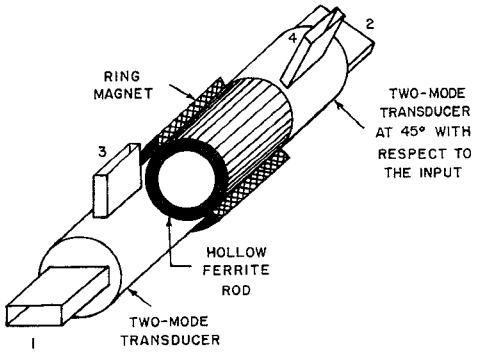

Fig. 11—Polarization-type circulator.

source was not available, the actual power required to cause the ferrite to lose its magnetic properties could not be determined. For 1000 watts input, the temperature of the ferrite was only 100°C as compared to its Curie temperature of 215°C. The insertion loss at this power level was approximately 0.7 db. Since it was found that the change in loss due to the increased temperature was less than 0.1 db, the 0.3 db increase in loss was attributed to the nonlinear attenuation characteristic of the ferrite. Sakiotis, Chait, and Kales[12] have shown that for power levels greater than about 1000 watts this characteristic becomes important. Under these conditions, the power handling capacity of the ferrite structure is limited not only by the heat dissipation but also by the power level at which the nonlinear effects become appreciable. Thus, from the above temperature data, it is doubtful if the circulator shown in Fig. 11 can retain its properties at cw powers of greater than 2000 watts.

A second type of ferrite circulator has been described by Hogan[1] which employs two magic-tees and a gyrator. This type is shown in Fig. 12. By using a hollow ferrite rod which has 90° rotation and a 90° twist section, a difference in phase shift of 180° for the two directions of propagation through the ferrite-twist combination can be obtained. Since any energy which enters port 1 splits between the two branches of the circulator, only half of the input power passes through the ferrite. Therefore, by using a 90° hollow rod section with the same inside and outside diameters as the one used in the 45° circulator, the high-power insertion loss between successive ports would still be 0.7 db while the power handling capacity should be doubled (*viz.*, 2000 watts).

[12] N. Sakiotis, H. N. Chait, and M. L. Kales, "Nonlinearity of propagation in ferrite media," PROC. IRE, vol. 43, p. 1011; August, 1955.

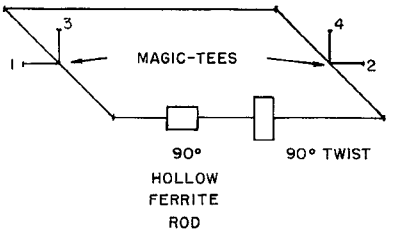

Fig. 12—Gyrator-type circulator.

Conclusion

The insertion loss and Faraday rotation for various ferrite configurations have been studied by use of a system capable of measuring microwave loss to within ± 0.05 db. By defining both a power handling and transmission figure of merit, a ferrite structure capable of handling large amounts of microwave power was chosen. With this structure a polarization type circulator was constructed with a power handling capacity of at least 1000 watts and an insertion loss of less than 0.7 db at the high-power level. In addition, a gyrator type circulator has been suggested which should have a 2000 watts power handling capacity with a high-power insertion loss of less than 0.7 db.

Appendix

When a ferrite is magnetized in the z direction, the rf components of $\vec{B}$ and $\vec{H}$ are related in the following manner:

$$\vec{B} = \mu\vec{H}_t + j\vec{K}\vec{i}_z \times \vec{H}_t + \mu_z\vec{H}_z\vec{i}_z \qquad (2)$$

where the subscript t denotes the projection of a vector on the xy plane and $\vec{i}_z$ denotes the unit vector in the z direction.

Assuming an $e^{j\omega t+\gamma z}$ dependency, Maxwell's equations may be written as follows:

$$\nabla_t \times \vec{E} + \vec{\gamma i}_z \times \vec{E} = -j\vec{\omega B}$$
$$\nabla_t \times \vec{H} + \vec{\gamma i}_z \times \vec{H} = j\omega\vec{\epsilon E}$$

where ϵ is the dielectric constant of the ferrite.

Using (2) and the divergence relations, the above equations may be rewritten in the following form:

$$\nabla_t^2 E_z + aE_z + bH_z = 0$$
$$\nabla_t^2 H_z + cH_z + dE_z = 0$$

where

$$a = g^2 - g_0^2\frac{K}{\mu}, \qquad b = -\omega\gamma K\frac{\mu_z}{\mu},$$
$$c = g^2\frac{\mu_z}{\mu}, \qquad d = \omega\gamma\epsilon\frac{K}{\mu}$$

and

$$g_0^2 \equiv \omega^2 K\epsilon \qquad g^2 \equiv \omega^2\mu\epsilon + \gamma^2.$$

Transforming the above equations into a pair of scalar wave equations we obtain

$$\nabla_t^2 u_1 + S_1 u_1 = 0$$
$$\nabla_t^2 u_2 + S_2 u_2 = 0 \tag{3}$$

where

$$E_z = S_1 u_1 + S_2 u_2$$
$$H_z = S_1 \frac{S_1 - a}{b} u_1 + S_2 \frac{S_2 - a}{b} u_2 \tag{4}$$

and

$$S_1 S_2 = ac - bd \qquad S_1 + S_2 = a + c.$$

Since u_1 and u_2 are related to E_z and H_z, and E_t and H_t are related to E_z and H_z through the curl relations, we can write E_t in terms of u_1 and u_2. These equations are

$$\vec{E}_t = \gamma \nabla_t (u_1 + u_2) - \frac{j\mu}{\gamma K} \vec{i}_z \times \nabla_t \{(S_1 - a)u_1 + (S_2 - a)u_2\}$$
$$\vec{H}_t = \frac{1}{\omega K} \nabla_t \{(g^2 - S_1)u_1 + (g^2 - S_2)u_2\}$$
$$- j\omega\epsilon \vec{i}_z \times \nabla_t (u_1 + u_2). \tag{5}$$

Since u_1 and u_2 are the solutions to (3), then (4) and (5) define the electromagnetic field in the ferrite region of a waveguide structure.

Because of the circular symmetry, we solve the scalar wave equations in cylindrical coordinates. Thus

$$u_1 = [A_1 J_n(\sqrt{S_1} r) + B_1 N_n(\sqrt{S_1} r)] e^{jn\phi}$$
$$u_2 = [C_1 J_n(\sqrt{S_2} r) + D_1 N_n(\sqrt{S_2} r)] e^{jn\phi}$$

where A_1, B_1, C_1, and D_1 are constants and J_n and N_n represent the Bessel functions of the first and second kind, respectively. In the waveguide region containing a homogeneous isotropic dielectric ϵ_2, the solution of the wave equation yields

$$E_{z_2} = [A_2 J_n(kr) + B_2 N_n(kr)] e^{jn\phi}$$
$$H_{z_2} = [C_2 J_n(kr) + D_2 N_n(kr)] e^{jn\phi}$$

where

$$k^2 = \gamma^2 + \omega^2 \mu_2 \epsilon_2.$$

Having the various field components, we can now solve for the propagation constants in ferrite structures similar to those in Fig. 1. Since the tangential components of E and H must be continuous across the boundary between the ferrite and the dielectric, this leads to four equations involving the field distribution in both the ferrite and dielectric regions. In order to obtain a nontrivial solution, we require that the determinant of their coefficients must equal zero. From this condition we obtain the equation which when solved yields the propagation constants for the various modes in the circularly-symmetric ferrite-loaded waveguide.

For the structure shown in Fig. 1(a) the equation is

$$P_1 Q_2 = P_2 Q_1 \tag{6}$$

where for $i = 1, 2$

$$P_i = \left[\left\{ \frac{\mu_2 \mu}{\mu_z K} S_i (S_i - a) r_1 G_1'(r_1) + n\gamma^2 (k^2 - S_i) G_1(r_1) \right\} J_n(\sqrt{S_i} r_1) - \frac{\mu}{K} k^2 (S_i - a) \sqrt{S_i} r_1 J_n'(\sqrt{S_i} r_1) G_1(r_1) \right]$$

$$Q_i = \left[\left\{ nF_1(r_1) \left[k^2 (g^2 - S_i) + \frac{\mu}{\mu_z} S_i (S_i - a) \right] + \omega^2 K \epsilon_2 S_i r_1 F_1'(r_1) \right\} J_n(\sqrt{S_i} r_1) - k^2 \omega^2 K \epsilon \sqrt{S_i} r_1 J_n'(\sqrt{S_i} r_1) F_1(r_1) \right]$$

and

$$F_1(r) \equiv \left\{ \frac{J_n(kr)}{J_n(kr_0)} - \frac{N_n(kr)}{N_n(kr_0)} \right\}.$$
$$G_1(r) \equiv \left\{ \frac{J_n(kr)}{J_n'(kr_0)} - \frac{N_n(kr)}{N_n'(kr_0)} \right\}.$$

$r_1 \equiv$ radius of the ferrite rod,

$r_0 \equiv$ radius of the circular waveguide.

In all these equations the primes signify differentiation with respect to the complete argument.

For the structure shown in Fig. 1(b), the eigenvalue equation is

$$P_1 Q_2 = P_2 Q_1 \tag{7}$$

where

$$P_1 \equiv \left\{ \begin{array}{l} [nK\mu_z\gamma^2(S_1 - k^2) J_n(kr_1) - \mu\mu_2 S_1 (S_1 - a) kr_1 J_n'(kr_1)] F(\sqrt{S_1} r_1) \\ + [nK\mu_z\gamma^2(S_2 - k^2) J_n(kr_1) - \mu\mu_2 S_2 (S_2 - a) kr_1 J_n'(kr_1)] m_3 N_n(\sqrt{S_2} r_1) \\ + \mu\mu_z k^2 r_1 J_n(kr_1) [\sqrt{S_1}(S_1 - a) F'(\sqrt{S_1} r_1) + \sqrt{S_2}(S_2 - a) m_3 N_n'(\sqrt{S_2} r_1)] \end{array} \right\}$$

$$P_2 \equiv \left\{ \begin{array}{l} [nK\mu_z\gamma^2(S_2 - k^2) J_n(kr_1) - \mu\mu_2 S_2 (S_2 - a) kr_1 J_n'(kr_1)] G(\sqrt{S_2} r_1) \\ + [nK\mu_z\gamma^2(S_1 - k^2) J_n(kr_1) - \mu\mu_2 S_1 (S_1 - a) kr_1 J_n'(kr_1)] m_2 N_n(\sqrt{S_1} r_1) \\ + \mu\mu_z k^2 r_1 J_n(kr_1) [\sqrt{S_2}(S_2 - a) G'(\sqrt{S_2} r_1) + \sqrt{S_1}(S_1 - a) m_2 N_n'(\sqrt{S_1} r_1)] \end{array} \right\}$$

$$Q_1 \equiv \left\{ \begin{array}{l} [n\{\mu S_1(S_1 - a) + \mu_z k^2(g^2 - S_1)\}J_n(kr_1) + \omega^2\epsilon_2 K\mu_z S_1 kr_1 J_n'(kr_1)]F(\sqrt{S_1}r_1) \\ + [n\{\mu S_2(S_2 - a) + \mu_z k^2(g^2 - S_2)\}J_n(kr_1) + \omega^2\epsilon_2 K\mu_z S_2 kr_1 J_n'(kr_1)]m_3 N_n(\sqrt{S_2}r_1) \\ - \omega^2\epsilon K\mu_z k^2 r_1 J_n(kr_1)[\sqrt{S_1}F'(\sqrt{S_1}r_1) + \sqrt{S_2}m_3 N_n'(\sqrt{S_2}r_1)] \end{array} \right\}$$

$$Q_2 \equiv \left\{ \begin{array}{l} [n\{\mu S_2(S_2 - a) + \mu_z k^2(g^2 - S_2)\}J_n(kr_1) + \omega^2\epsilon_2 K\mu_z S_2 kr_1 J_n'(kr_1)]G(\sqrt{S_2}r_1) \\ + [n\{\mu S_1(S_1 - a) + \mu_z k^2(g^2 - S_1)\}J_n(kr_1) + \omega^2\epsilon_2 K\mu_z S_1 kr_1 J_n'(kr_1)]m_2 N_n(\sqrt{S_1}r_1) \\ - \omega^2\epsilon K\mu_z k^2 r_1 J_n(kr_1)[\sqrt{S_2}G'(\sqrt{S_2}r_1) + \sqrt{S_1}m_2 N_n'(\sqrt{S_1}r_1) \end{array} \right\}$$

and

$$F(\sqrt{S_1}r) \equiv J_n(\sqrt{S_1}r) + m_1 N_n(\sqrt{S_1}r), \qquad G(\sqrt{S_2}r) \equiv J_n(\sqrt{S_2}r) + m_4 N_n(\sqrt{S_2}r)$$

$$m_1 \equiv \frac{\left\{ \begin{array}{l} [S_1 J_n(\sqrt{S_1}r_0)]\left[\frac{n\gamma}{r_0} N_n(\sqrt{S_2}r_0) - \frac{\mu}{\gamma K}\sqrt{S_2}(S_2 - a)N_n'(\sqrt{S_2}r_0)\right] \\ - [S_2 N_n(\sqrt{S_2}r_0)]\left[\frac{n\gamma}{r_0} J_n(\sqrt{S_1}r_0) - \frac{\mu}{\gamma K}\sqrt{S_1}(S_1 - a)J_n'(\sqrt{S_1}r_0)\right] \end{array} \right\}}{\left\{ \begin{array}{l} [S_2 N_n(\sqrt{S_2}r_0)]\left[\frac{n\gamma}{r_0} N_n(\sqrt{S_1}r_0) - \frac{\mu}{\gamma K}\sqrt{S_1}(S_1 - a)N_n'(\sqrt{S_1}r_0)\right] \\ - [S_1 N_n(\sqrt{S_1}r_0)]\left[\frac{n\gamma}{r_0} N_n(\sqrt{S_2}r_0) - \frac{\mu}{\gamma K}\sqrt{S_2}(S_2 - a)N_n'(\sqrt{S_2}r_0)\right] \end{array} \right\}}$$

$$m_2 \equiv \frac{\left\{ \begin{array}{l} [S_2 J_n(\sqrt{S_2}r_0)]\left[\frac{n\gamma}{r_0} N_n(\sqrt{S_2}r_0) - \frac{\mu}{\gamma K}\sqrt{S_2}(S_2 - a)N_n'(\sqrt{S_2}r_0)\right] \\ - [S_2 N_n(\sqrt{S_2}r_0)]\left[\frac{n\gamma}{r_0} J_n(\sqrt{S_2}r_0) - \frac{\mu}{\gamma K}\sqrt{S_2}(S_2 - a)J_n'(\sqrt{S_2}r_0)\right] \end{array} \right\}}{\left\{ \begin{array}{l} [S_2 N_n(\sqrt{S_2}r_0)]\left[\frac{n\gamma}{r_0} N_n(\sqrt{S_1}r_0) - \frac{\mu}{\gamma K}\sqrt{S_1}(S_1 - a)N_n'(\sqrt{S_1}r_0)\right] \\ - [S_1 N_n(\sqrt{S_1}r_0)]\left[\frac{n\gamma}{r_0} N_n(\sqrt{S_2}r_0) - \frac{\mu}{\gamma K}\sqrt{S_2}(S_2 - a)N_n'(\sqrt{S_2}r_0)\right] \end{array} \right\}}$$

$$m_3 \equiv \frac{\left\{ \begin{array}{l} [S_1 N_n(\sqrt{S_1}r_0)]\left[\frac{n\gamma}{r_0} J_n(\sqrt{S_1}r_0) - \frac{\mu}{\gamma K}\sqrt{S_1}(S_1 - a)J_n'(\sqrt{S_1}r_0)\right] \\ - [S_1 J_n(\sqrt{S_1}r_0)]\left[\frac{n\gamma}{r_0} N_n(\sqrt{S_1}r_0) - \frac{\mu}{\gamma K}\sqrt{S_1}(S_1 - a)N_n'(\sqrt{S_1}r_0)\right] \end{array} \right\}}{\left\{ \begin{array}{l} [S_2 N_n(\sqrt{S_2}r_0)]\left[\frac{n\gamma}{r_0} N_n(\sqrt{S_1}r_0) - \frac{\mu}{\gamma K}\sqrt{S_1}(S_1 - a)N_n'(\sqrt{S_1}r_0)\right] \\ - [S_1 N_n(\sqrt{S_1}r_0)]\left[\frac{n\gamma}{r_0} N_n(\sqrt{S_2}r_0) - \frac{\mu}{\gamma K}\sqrt{S_2}(S_2 - a)N_n'(\sqrt{S_2}r_0)\right] \end{array} \right\}}$$

$$m_4 = \frac{\left\{ \begin{array}{l} [S_1 N_n(\sqrt{S_1}r_0)]\left[\frac{n\gamma}{r_0} J_n(\sqrt{S_2}r_0) - \frac{\mu}{\gamma K}\sqrt{S_2}(S_2 - a)J_n'(\sqrt{S_2}r_0)\right] \\ - [S_2 J_n(\sqrt{S_2}r_0)]\left[\frac{n\gamma}{r_0} N_n(\sqrt{S_1}r_0) - \frac{\mu}{\gamma K}\sqrt{S_1}(S_1 - a)N_n'(\sqrt{S_1}r_0)\right] \end{array} \right\}}{\left\{ \begin{array}{l} [S_2 N_n(\sqrt{S_2}r_0)]\left[\frac{n\gamma}{r_0} N_n(\sqrt{S_1}r_0) - \frac{\mu}{\gamma K}\sqrt{S_1}(S_1 - a)N_n'(\sqrt{S_1}r_0)\right] \\ - [S_1 N_n(\sqrt{S_1}r_0)]\left[\frac{n\gamma}{r_0} N_n(\sqrt{S_2}r_0) - \frac{\mu}{\gamma K}\sqrt{S_2}(S_2 - a)N_n'(\sqrt{S_2}r_0)\right] \end{array} \right\}}.$$

r_1 = inside radius of the ferrite cylinder,

$r_0 \equiv$ radius of the circular waveguide.

Solving (6) and (7) for $n = \pm 1$ yields the circularly polarized propagation constants for the modified TE_{11} mode. Then by use of (1), the saturation rotation can be obtained for the composite ferrite and dielectric structures shown in Fig. 1.

Some of these theoretical results are given in Fig. 2 and Fig. 3.

ACKNOWLEDGMENT

The author wishes to express his sincere appreciation to Prof. F. J. Beck for his valuable advice during the course of this investigation. He also wishes to acknowledge his indebtedness to various members of the Microwave Group, Missile Systems Division, Raytheon Manufacturing Company, for their valuable help.

Spectral Distribution of Thermal Noise in a Gas Discharge*

SAUL M. BERGMANN†

Summary—**By means of thermodynamic considerations it is shown under which conditions microwave noise power generated by a gas discharge can be considered thermal. A critical analysis of Mumford's hypothesis is made.**

INTRODUCTION

MUMFORD [1] has pointed out that a fluorescent lamp filled with argon at 2-mm pressure and a drop of mercury having a saturated pressure of 6–8 microns, can be used as a standard microwave noise source having an equivalent temperature of 11,400°K. By considering the case of a black body radiating at a temperature of 11,400°K, and calculating from Wien's displacement law the wavelength of maximum radiation at this temperature, Mumford found $\lambda_m = 2535$Å. The fact that an intensive mercury line lies at 2537Å led Mumford to postulate that in a gaseous discharge, radiating light energy substantially at one particular wavelength λ, the microwave noise power available is the same as that available from a black body radiating maximum power at that wavelength. In this paper, it is shown under which conditions the noise power generated by a gas discharge can be considered thermal. To this end a critical analysis of Mumford's hypothesis is made. Three broad lines of attack are open.

1) A general quantitative formulation of the frequency spectrum distribution of the gas discharge from the far ultraviolet region down to the microwave range, on a kinetic theory basis. A theoretical treatment has been made by Parzen and Goldstein [2], but by invoking some critical arguments put forth by van der Ziel [3] it can be shown that their results hold only for microwave frequencies and would not hold for higher ones. The general treatment however is very difficult.
2) An experimental investigation.
3) An approach based on thermodynamical considerations which can be dealt with semiquantitatively. This course will be followed in this treatment.

* Manuscript received by the PGMTT, December 19, 1956; revised manuscript received, June 3, 1957.
† Raytheon Mfg. Co., Waltham, Mass.

THERMODYNAMIC THEORY OF THERMAL NOISE IN A GAS DISCHARGE

Mumford's hypothesis can be reformulated by dividing it into two parts.

1) In a gaseous discharge the microwave noise power available is the same as that available from a black body at a particular temperature, T.
2) That particular temperature, T, is of such magnitude as to correspond to a maximum power radiation at a wavelength λ_m at which light energy is radiated substantially monochromatically.

Consider a cavity with walls perfectly reflecting at all frequencies.

Let the cavity contain particles with Maxwellian distribution of velocities and in thermal equilibrium with radiation present in it. It has been shown by Einstein [4] that the radiation energy density in the cavity will then follow Planck's radiation law

$$U_\nu d\nu = (8\pi h\nu^3/c^3)[\exp(h\nu/\kappa T) - 1]^{-1} \cdot d\nu \qquad (1)$$

where T corresponds to the temperature of the particles.

Planck has shown [5], that if some carbon dust or any other material, capable of reaching high temperatures without absorbing too much heat, is brought into a perfectly reflecting cavity containing radiation, the radiation will redistribute itself and follow (1) after thermal equilibrium has been established. The temperature T will then be that of the material agent. Thus, if the cavity originally contained sharp mercury lines those would be absorbed, and partially re-emitted, and the radiation energy density would eventually obey (1).

Consider a gas discharge tube in a waveguide in a